Remote photonic sensing of glucose concentration via analysis of time varied speckle patterns

Nisan Ozana[1], Roy Talman[1], Amir Shemer[1], Ariel Schwartz[1], Sagi Polani[2], Ran Califa[2], Yevgeny Beiderman[2], Joaquin Ruiz-Rivas[2], Javier García[3] and Zeev Zalevsky[1*]

[1]*Faculty of Engineering and the Nano Technology Center, Bar-Ilan University, Ramat-Gan 52900, Israel*
[2]*ContinUse Biometrics Ltd., HaBarzel 32b st., Tel Aviv 6971048, Israel*
[3]*Departamento de Óptica, Universitat de València, C/Dr. Moliner 50, 46100 Burjassot, Spain*

*Corresponding author

DOI: 10.5185/amlett.2018.2054
www.vbripress.com/aml

Abstract

The ability to perform a remote sensing of glucose in the blood stream can be very applicable. The novel method presented in this paper is based on two optical approaches both based on the extraction and analysis of the changes in the collected speckle field. The first physical effect used for the detection is the temporal changes of the back scattered secondary speckles produced in the skin due to the changes of the blood stream parameters as a function of the glucose concentration in the blood. These cardio related changes can be analyzed with different machine learning algorithms to enhance the sensitivity of the measurements. The second physical effect assisting in performing the remote glucose sensing is the Faraday rotation effect in which the polarization of linearly polarized light is rotated when scattered from materials exhibiting this effect while being exposed to a magnetic field. Copyright © 2018 VBRI Press.

Keywords: Sensors, speckles; glucose concentration detection.

Introduction

Noninvasive glucose monitoring refers to the measurement of blood glucose levels without drawing blood, puncturing the skin, or causing pain or trauma to the patient. Most of noninvasive glucose monitoring methods are based on measuring blood glucose using transdermal measurements. These methods attempt to pull glucose through the interstitial fluid using either chemicals, electricity or ultrasound. The interstitial fluid, which surrounds cells including those of the skin and provides a reservoir of nutrients including glucose, is very close to the exterior of the body, only 0.01mm below the surface of the skin. Thus, absorption of infra-red light, may allow measuring glucose levels [1].

As of 2014, there have been very few noninvasive glucose meters, that are being marketed in several countries. Measurement of glucose levels in interstitial fluid is currently available in the form of continuous glucose monitors (CGMs), however, these are invasive devices which require having a sensor implanted below the surface of the skin.

The search for noninvasive glucose monitoring began after 1975 and has continued till present days without a clinically or commercially viable product. As of 1999, only one such product, the GlucoWatch automatic glucose biographer (Cygnus Inc), had ever been approved for sale by the FDA. It was based on a technique for electrically pulling glucose through intact skin. It was withdrawn after a short time owing to poor performance and some damage to the skin [2].

One major method for remote monitoring of glucose is infrared spectroscopy [3]. This method measures glucose through the skin using light of slightly longer wavelengths than the visible region. It is based on using transdermal measurement for measuring the amount of polarized light that is rotated by glucose in the front chamber of the eye (containing the "aqueous humor"). Other examples include bio-impedance spectroscopy [4], electromagnetic sensing [5], fluorescence technology [6], mid-infrared spectroscopy [7], optical coherence tomography [8], optical polarimetry [9], Raman spectroscopy [10], ultrasound technology [11] and photoacoustic spectroscopy [12]. Concluding with the observation that none of these had produced a well commercially, clinically reliable device and therefore, much work remained to be done.

In this paper, using a new and patented approach [13-15], we present a new technique for remote measuring of glucose. The described method includes a combination of 2 different effects. The first indirect effect consists of illumination of the human skin, which is close to a blood artery, with a laser beam. The back scattered light from the skin near the blood artery creates a secondary speckle patterns. These self-interference random patterns (i.e. speckle patterns) movement are due to the blood pulse stream changes that can be extracted [16 - 20]. Various bio-parameters can be monitored from the blood flux pulsation. Using machine learning algorithms and trading process of the detected signals, the glucose concentration can be extracted. The second direct effect includes the Faraday rotation effect which is the rotation of the plane of vibration of linearly polarized light when passing through a medium exhibiting this effect [21]. Changing the polarization state of the wavefront will cause the speckle patterns to change as shown in Ref. [22]. To minimize the mechanical noise, short magnetic pulses in a sense of mechanical rise time were generated. The innovation presented in this magneto – optic effect is the AC short pulses of the magnetic field that can better isolate the signal related to the glucose form the noise associated with the natural mechanical vibrations of the setup. Thus, in addition to other proved effects, this technique increases the observability of the relatively small magneto-optic effect.

Remote indirect optical measurement of glucose concentration

Theoretical explanation

The optical setup consisted of: (a) an eye safe 780nm laser and (b) a camera (Basler acA1920-25um, monochrome). The camera captures the speckle images at 300 frames per second (fps). The distance from the laser to the subject's leg was approximately 90cm. First, a big spot pattern was illuminated on the subject's leg. Later, the big spot was divided to 25 spatial sub-spots to perform the numerical analysis. Mathematically the light distribution can be expressed as follows:

$$A(x_0, y_0) = \left| \int\int \exp[i\phi(x,y)] \exp\left[i(\beta_x x + \beta_y y)\right] \exp\left[\frac{\pi i}{\lambda Z}\left((x-x_0)^2 + (y-y_0)^2\right)\right] dxdy \right| \quad (1)$$

where ϕ is the random phase generated by the skin roughness, λ is the illuminated wavelength (532nm) and Z is the axial distance to the imaging plane. β expresses the skin tilting movement due to blood pulse stream:

$$\beta = \frac{4\pi \tan\alpha}{\lambda} \quad (2)$$

where α is the skin tilting angle. To sense the tilting movement, the image captured by the camera was strongly defocused. Thus, the imaging plane was moved to the far field regime as explained in Ref [13], therefore, the tilting movement can be expressed as follows:

$$A(x_0, y_0) = \left| \int\int \exp[i\phi(x,y)] \exp\left[i(\beta_x x + \beta_y y)\right] \exp\left[\frac{-2\pi i}{\lambda Z}(xx_0 + yy_0)\right] dxdy \right| \quad (3)$$

Using a simple correlation based algorithm, the 2-D movement of the blood vessels can be extracted. Temporal movement of the reflecting surface causes changes to the random speckle pattern over time due to the temporal change in its tilting angle. In the first step, a set of images as a function of time was captured. In the second step, the sequential 2-D row data is correlated. The relative movement of patterns can be extracted using a 2-D correlation. The position of the correlation peak over time expresses this relative tilting movement. The temporal movement of the speckle is caused by the blood flow changes. This signal presents an optical phonocardiogram (OPG) signal as shown in **Fig. 1**.

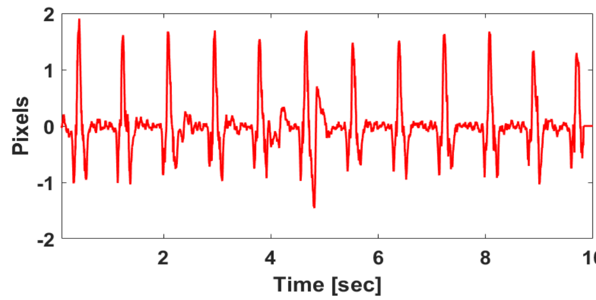

Fig. 1. An example for an OPG signal from the leg.

The next step is to use the map of the OPG signals (5x5) as shown in **Fig. 2** for machine learning algorithms such as random forest to extract the glucose concentration trend. Summary of the presented process is presented in **Fig. 3**.

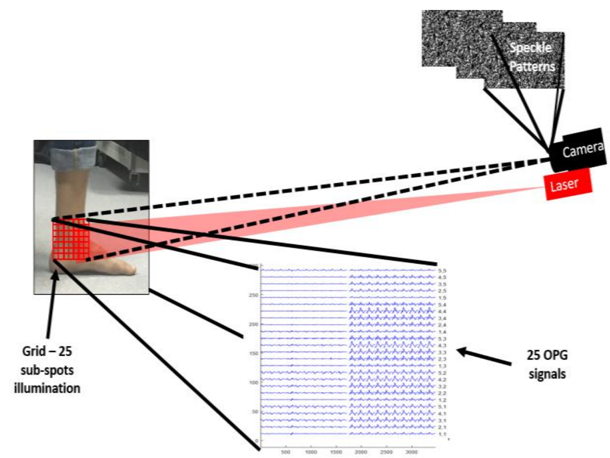

Fig. 2. Schematic sketch of the presented configuration.

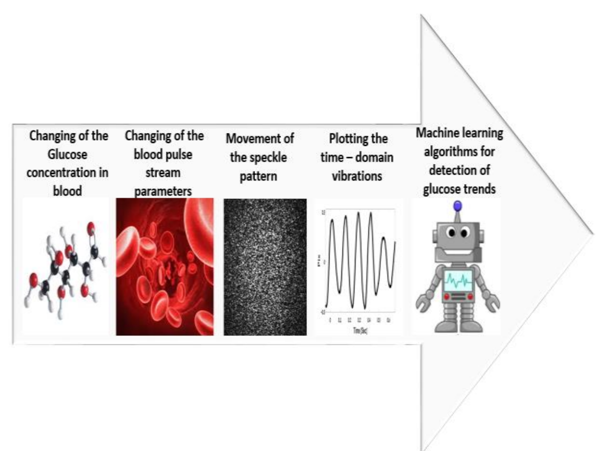

Fig. 3. Summary of the presented process.

Machine learning analysis

Glucose levels were taken from the subject after 12 hours of fasting. The units of glucose concentration levels are given as mg/dl, hence a calibration between the optical reults to the reference device was calculated. In this experiment the sensor was measuring the back reflected patterens from the subject's leg main blood artery area. To retain only signals of good quality, pre-processing recordings were preprocessed. Each 10 minutes, a blood sample from a finger was taken to measure the glucose concentration with a glucometer (FreeStyle Lite Blood Glucose Monitoring System). First, the subject was measured with the optical method as well as with the reference device before drinking a sweetend drink. Afterwards the subject drank 500 ml of a sweetened drink. The ingredients of this drink are shown in **Table 1**.

Table 1. Nutritional ingredients of the sweetened drink.

	Quantity	Units
Energy	195	Calories
Carbohydrates	50	G
Sodium	50	mg
Vitamin C	30	mg

During the tests, 5 different levels of glucose were measured. During the first step of the machine learning procecing using random forest alghorithem, a training of the alghorethem was performed. During the tests, 10% of the samples from each glucose level was randomally chosen for training using random forest clasifier with 50 trees. Later, using the training process, the signals were tested to predict the glucose concentration value. One can see in **Fig. 4** the predication of each illuminating laser spot seperatly. The percentage of each spot OPG good quality signals is also shown in the following **Fig. 4**.

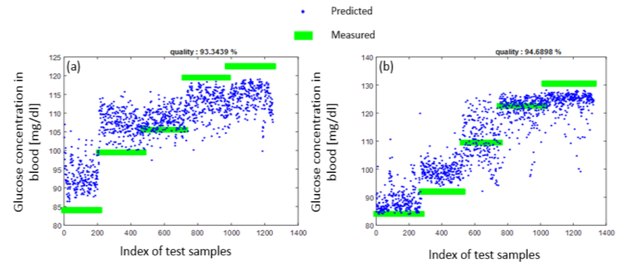

Fig. 5. Two tests of glucose prediction using the presented method. The tests are denoted by (a) and (b). The graphs show predicted values denoted by blue dots with respect to real glucose values denoted by green lines.

Summary of 2 glucose test are shown in **Fig. 5**. These tests include all the test samples from all of the spots. The percentage of the signals that passed the quality test is also shown in **Fig. 5**. One can see the good predication using the presented method.

During the second part **(Fig. 6)** of these tests, the subject drank the same amount of water without glucose. Is is shown that during the first test (i.e glucose test) there is an increase in the measured distribution corresponding to real value of the glucose concentration in the blood stream. However, as expected, during the second experiment (i.e. the water test) there is no change of the predicted values. The aim of the water test is to demonstrate that the technique is not effected by the changes in the volume of the blood, due to the addition of the drinking water, but rather the variation sin the measured values are indeed due to the modification in the glucose level in the blood stream.

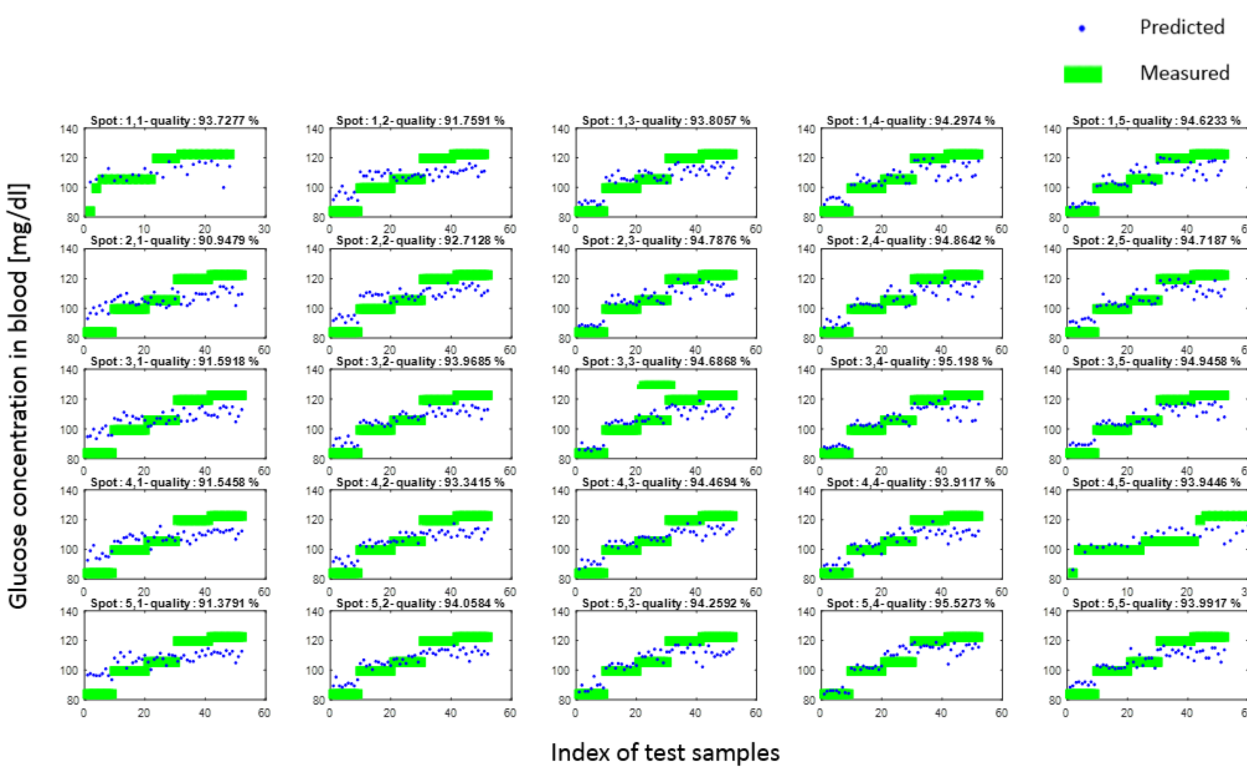

Fig. 4. A prediction map of each spatial illuminating laser spot. Each spot presents a different location next to the subject's leg main blood artery. The graphs show predicted values denoted by blue dots with respect to real glucose values denoted by green lines.

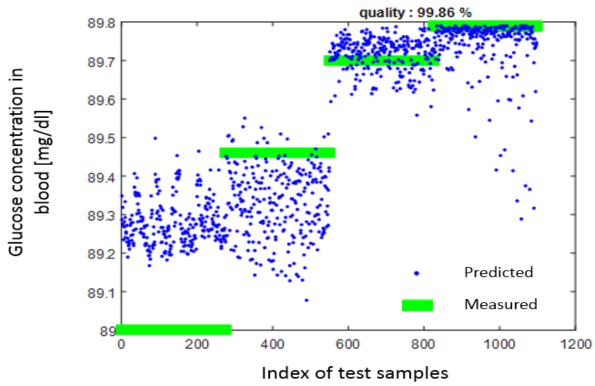

Fig. 6. A graph of a water test. During this test, the subject drank only water without glucose. The graph shows predicted values denoted by blue dots with respect to real glucose values denoted by green lines.

Remote optical measurement of glucose concentration – magneto-optic effect

Theoretical explanation

As shown in Ref. [22], a change of a wavefront polarization state can be caused by the glucose concentration changes. In magneto-optic materials polarization will be rotated according to the following expression:

$$\theta = \vartheta BL = {}^{\pi L \Delta n(B)}\!/_{\lambda} \quad (4)$$

Where ϑ is Verdet constant, B is the magnetic field and L is the interaction length, λ is the optical wavelength and Δn is the difference in the index of refraction between two circularly polarized states leading to the rotation. Verdet constant is defined as [23]:

$$V = \frac{\alpha}{l \cdot H \cdot \cos(\varphi)} \quad (5)$$

while α is the angular rotation, l is the length path through the substance, H is the intensity of the magnetic field and φ is the angle between the magnetic field and the path of the light. As proven in Ref. [22] the minimal magnetic field *Bmin* that will de-correlate the speckle field is proportional to:

$$B_{\min} \propto \pi L \theta R \quad (6)$$

while R is the radius of the illuminating beam and L is the interaction length. It was shown in Ref. [15] that sensitivity of the glucose measurement can also be improved with an AC magnetic field due to the lock-in amplification while magnetic square wave at specific frequency was generated. However, the main disadvantage of this method is the vibrations noise at the same frequency of the magnetic field. To enhance the sensitivity of our measurement, a magnetic field with short pulses was generated. These short pulses are smaller than the rise time of the mechanical vibrations but bigger than the rise time of the magnetic field. Schematic sketch of the pulse design is shown in the following **Fig. 7**. The aim of this innovation is to increase the SNR of the measured signal.

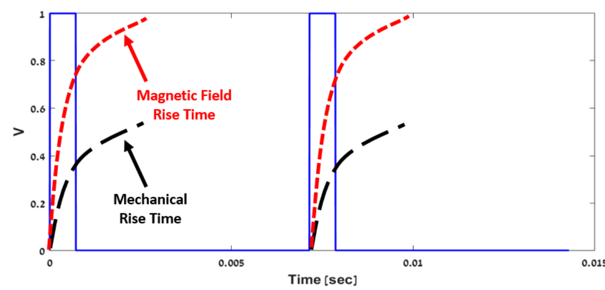

Fig. 7. Short pulses generation with respect to the mechanical rise time.

Multiple linear regression method

The experimental optical remote configuration is shown in **Fig. 8**. The configuration consists of a camera (PixelLink PL-E531) which captures images of the time varied speckle patterns at 2000 fps, an eye safe 532nm laser, a polarizer and a filter. The coil generated magnetic short pulses of 1ms at 120Hz and the detected AC magnetic field was at strength of 100 Gauss (measured by Gaussmeter, AlphaLab, GM2). Each glucose sample consisted of 1% of intra lipid (IL), 1% of agarose and different concentrations of glucose. Each glucose sample was made in a cuvette that was inserted inside the coil.

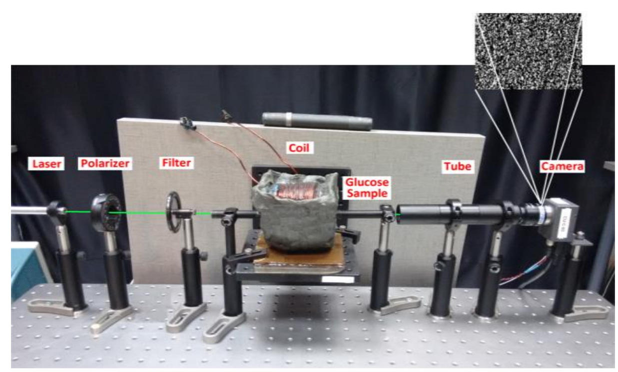

Fig. 8. The remote configuration for the magneto optic effect.

One can see in **Fig. 9** an example for the frequency response corresponding to 1ms sec magnetic field pulses at repetition rate of 120Hz (the pulses are shown in Fig. 7). The frequency response is presented in the Y axis in pixels units (shifts of the speckle pattern in cameras pixels units).

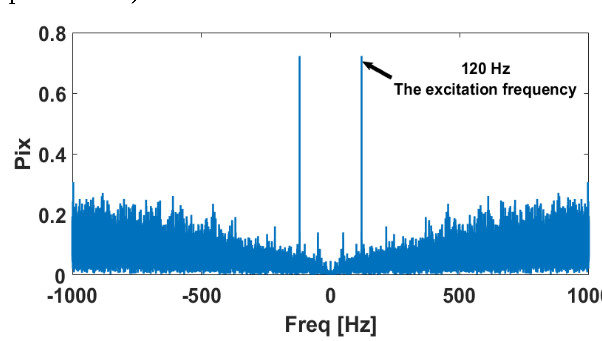

Fig. 9. The frequency response of 1ms magnetic pulses at a repetition rate of 120Hz.

To extract the glucose concentration value, a multiple linear regression processing was used. This process was calculated according to the equations presented in Ref. [24]. During these measurements, 5 different glucose concentrations were examined: 1%, 0.5%, 0.25%, 0.15% and 0.05%. Each sample was measured 3 times. For this calculation, the frequency response of X axis and Y axis at the excitation frequency were calculated during this process. The results are shown in Fig. 10. One can see the predicted value according to the suggested regression process.

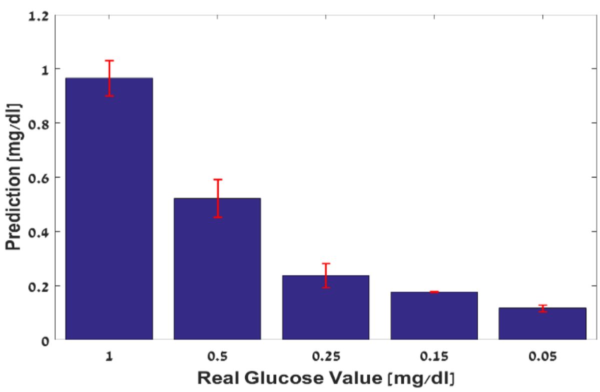

Fig. 10. The glucose prediction values according to multiple linear regression process.

Conclusions

This paper presents the first steps towards developing a module for continuous and non-invasive detection of glucose concentration trends using two approaches. The first one is an indirect approach, that extracts the glucose trends via the blood stream changes while applying machine learning algorithms. The aim of the second approach is to find a direct effect of the glucose on the detected speckle pattern using magneto-optical phenomena. This paper shows the ability to extract a frequency response at the excitation frequency using low mechanical noises. However, this approach decreases the magnetic field, therefore, a configuration with high magnetic field and low acoustic noise should be designed. Translation of the optical readout into the exact value of the estimated biomedical parameter using a robust device is also required. The glucose test showed the preliminary feasibility of detecting trends in the glucose concertation remotely with low acoustic noise.

References

1. G. Danaei, M. M. Finucane, Y. Lu, G. M. Singh, M. J. Cowan and C. J. Paciorek, "National, regional, and global trends in fasting plasma glucose and diabetes prevalence since 1980," The Lancet **378**, 31-40.
2. J.A. Tamada, S. Garg, L. Jovanovic, K.R. Pitzer, S. Fermi, R.O. Potts, "Noninvasive glucose monitoring: comprehensive clinical results. Cygnus Research Team". JAMA. 282 (19): 1839-44 (1999)
3. A. Tura, A. Maran, and G. Pacini, "Non-invasive glucose monitoring: Assessment of technologies and devices according to quantitative criterion," Elsevier J. of Diabetes Research and Clinical Practice, vol. 77, no. 6, pp. 16-40, 2007.
4. Chi-Fuk et al. "Recent Advances in Noninvasive Glucose Monitoring." Medical Devices (Auckland, N.Z.) 5 (2012): 45–52. PMC. Web. 19 Jan. 2018.
5. M. Hofmann, M. Bloss, R. Weigel, G. Fischer and D. Kissinger, "Non-invasive glucose monitoring using open electromagnetic waveguides," 2012 42nd European Microwave Conference, Amsterdam, 546-549 (2012).
6. D. Klonoff, Overview of Fluorescence Glucose Sensing: A Technology with a Bright Future. Journal of Diabetes Science and Technology. 6. 1242-50 (2012).
7. P. Bhandare, Y. Mendelson, R. Peura, G. Janatsch, J. Kruse-Jarres, R. Marbach, and H. Heise, "Multivariate Determination of Glucose in Whole Blood Using Partial Least-Squares and Artificial Neural Networks Based on Mid-Infrared Spectroscopy," Appl. Spectrosc. 47, 1214-1221 (1993).
8. R. O. Esenaliev, K. V. Larin, I. V. Larina, and M. Motamedi, "Noninvasive monitoring of glucose concentration with optical coherence tomography," Opt. Lett. **26**, 992-994 (2001).
9. A. Winkler, G. Bonnema, and J. Barton, "Optical polarimetry for noninvasive glucose sensing enabled by Sagnac interferometry," Appl. Opt. 50, 2719-2731 (2011).
10. C. Pelletier, J. Lambert, and M. Borchert, "Determination of Glucose in Human Aqueous Humor Using Raman Spectroscopy and Designed-Solution Calibration," Appl. Spectrosc. 59, 1024-1031 (2005).
11. L. Zhu, J. Lin, B. Lin, and H. Li, "Noninvasive blood glucose measurement by ultrasound-modulated optical technique," Chin. Opt. Lett. 11, 021701- (2013).
12. H. A. MacKenzie, H. S. Ashton, S. Spiers, Y. Shen, S. E. Freeborn, J. Hannigan, J. Lindberg and P. Rae, "Advances in Photoacoustic Noninvasive Glucose Testing," Clin Chem **45**, 1587–1595(1999).
13. Z. Zalevsky, Y. Beiderman, I. Margalit, S. Gingold, M. Teicher, V. Mico and J. Garcia, "Simultaneous remote extraction of multiple speech sources and heart beats from secondary speckles pattern," Opt. Express **17**, 21566-21580 (2009).
14. N. Ozana, N. Arbel, Y. Beiderman, V. Mico, M. Sanz, J. Garcia, A. Anand, B. Javidi, Y. Epstein, and Z. Zalevsky, "Improved noncontact optical sensor for detection of glucose concentration and indication of dehydration level," Biomed. Opt. Express 5, 1926-1940 (2014).
15. N. Ozana, Y. Beiderman, A. Anand, B. Javidi, S. Polani, A. Schwarz, A. Shemer, J. García-Monreal, and Z. Zalevsky, "Noncontact speckle-based optical sensor for detection of glucose concentration using magneto-optic effect," J. Biomed. Opt. 21(6) 065001 (2016).
16. Y. Beiderman, I. Horovitz, N. Burshtein, M. Teicher, J. Garcia, V. Mico and Z. Zalevsky, "Remote estimation of blood pulse pressure via temporal tracking of reflected secondary speckles pattern," J. of Biomedical Optics 15, 061707-1 - 061707-7 (2010).
17. Y. Beiderman, R. Talyosef, D. Yeori, J. Garcia, V. Mico and Z. Zalevsky, "The usage of PC mouse components for continuous measuring of human heart beats," Appl. Opt. 51, 3323-3328 (2012).
18. Y. Beiderman, M. Teicher; J. Garcia, V. Mico and Z. Zalevsky, "Optical technique for classification, recognition and identification of obscured objects," Opt. Commun. 283, 4274-4282 (2010).
19. N. Ozana, I. Margalith, Y. Beiderman, M. Kunin, G. Abebe Campino, R. Gerasi, J. Garcia, V. Mico and Z. Zalevsky, "Demonstration of a remote optical measurement configuration that correlates with breathing, heart rate, pulse pressure, blood coagulation and blood oxygenation," Proceedings of the IEEE 103, 248 - 262 (2015). (invited paper).
20. N. Ozana, Y. Bishitz, Y. Beiderman, J. Garcia and Z. Zalevsky, "Remote optical configuration of pigmented lesion detection and diagnosis of bone fractures," Proc. SPIE 9689, Photonic Therapeutics and Diagnostics XII, 968916 (2016).
21. M. J. Frieser, "A survey of magnetooptic effects," Magnetics, IEEE Trans **4**, 152–161 (1968).
22. A. Anand, V. Trivedi, S. Mahajan, V. K. Chhaniwal, Z. Zalevsky and B. Javidi, "Speckle-Based Optical Sensor for Low Field Faraday Rotation Measurement," Sensors Journal, IEEE **13**, 723-727(2013).
23. E. W. Washburn, International Critical Tables of Numerical Data, Physics, Chemistry and Technology, Norwich (2003).

24. S. H. Brown, “Multiple linear regression analysis: A matrix approach with MATLAB,” Alabama Journal of Mathematics, 1-3 (2009).

